REGULAR ARTICLE

blood advances

Erythrocyte β spectrin can be genetically targeted to protect mice from malaria

Patrick M. Lelliott,[1] Hong Ming Huang,[1] Matthew W. Dixon,[2] Arman Namvar,[2,3] Adam J. Blanch,[2] Vijay Rajagopal,[3] Leann Tilley,[2] Cevayir Coban,[4] Brendan J. McMorran,[1] Simon J. Foote,[1] and Gaetan Burgio[1]

[1]Department of Immunology and Infectious Disease, John Curtin School of Medical Research, Australian National University, Canberra, ACT, Australia; [2]Department of Biochemistry and Molecular Biology, Bio21 Molecular Science and Biotechnology Institute, and [3]Department of Biomedical Engineering, University of Melbourne, Melbourne, VIC, Australia; and [4]Laboratory of Malaria Immunology, Immunology Frontier Research Center, Osaka University, Osaka, Japan

Key Points

- Mutations in β spectrin cause microcytosis, resulting in increased clearance of erythrocytes and enhanced resistance to malaria in mice.
- A homozygous CRISPR/Cas9-induced mutation in the binding site between β spectrin and ankyrin-1 increases mouse survival during malaria.

The malaria parasite hijacks host erythrocytes to shield itself from the immune system and proliferate. Red blood cell abnormalities can provide protection from malaria by impeding parasite invasion and growth within the cell or by compromising the ability of parasites to avoid host clearance. Here, we describe 2 *N*-ethyl-*N*-nitrosourea–induced mouse lines, *Sptb*^{MRI26194} and *Sptb*^{MRI53426}, containing single-point mutations in the erythrocyte membrane skeleton gene, β spectrin (*Sptb*), which exhibit microcytosis but retain a relatively normal ratio of erythrocyte surface area to volume and are highly resistant to rodent malaria. We propose the major factor responsible for malaria protection is the specific clearance of mutant erythrocytes, although an enhanced clearance of uninfected mutant erythrocytes was also observed (ie, the bystander effect). Using an in vivo erythrocyte tracking assay, we established that this phenomenon occurs irrespective of host environment, precluding the involvement of nonerythrocytic cells in the resistance mechanism. Furthermore, we recapitulated this phenotype by disrupting the interaction between ankyrin-1 and β spectrin in vivo using CRISPR/Cas9 genome editing technology, thereby genetically validating a potential antimalarial target. This study sheds new light on the role of β spectrin during *Plasmodium* infection and highlights how changes in the erythrocyte cytoskeleton can substantially influence malaria susceptibility with minimal adverse consequences for the host.

Introduction

Malaria has exerted the strongest known selective pressure in the recent history of the human genome.[1] One of the outcomes of this is a higher prevalence of erythrocytic polymorphisms, which provides protection against malaria infection.[2,3] Studies of the biological mechanisms underlying this protection have led to an increased understanding of the interactions between host and parasite. For example, genetic polymorphisms such as Duffy negativity and glycophorin C null mutations, which impair parasite invasion, have facilitated the identification of parasite proteins involved in this process.[4-6] Studies of other erythrocyte polymorphisms have shown them to be associated with impaired cytoadherence of infected cells,[7,8] reduced erythrocyte rosetting,[9] enhanced phagocytosis of infected cells,[10,11] interference with parasite protein trafficking,[12] and modulation of parasite protein translation through microRNAs.[13] Mechanisms of resistance in these conditions are multifactorial and diverse and remain incompletely understood.

Submitted 8 June 2017; accepted 31 October 2017. DOI 10.1182/bloodadvances.2017009274.

The full-text version of this article contains a data supplement.

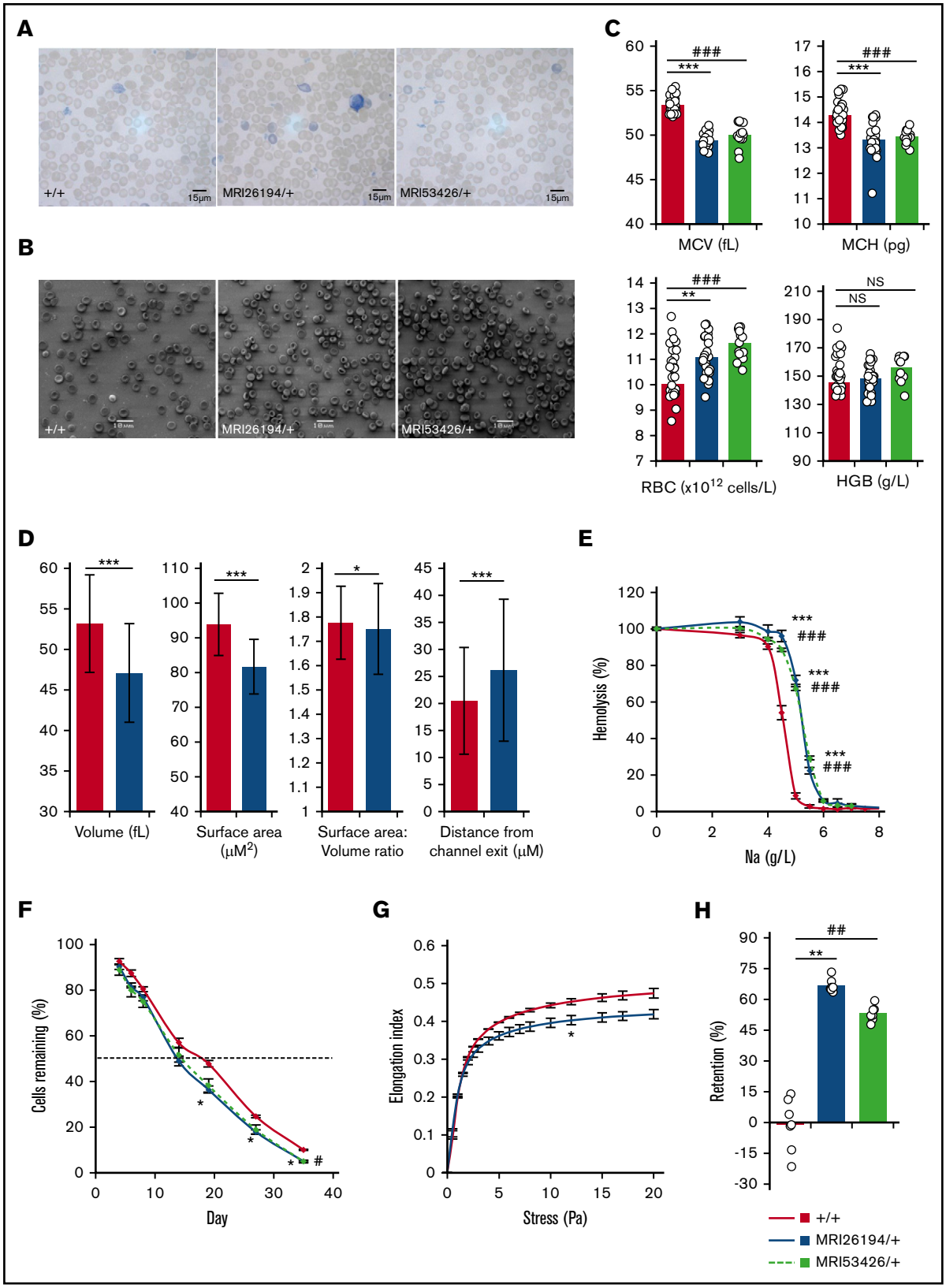

Figure 1. Hematological properties of mutant lines MRI26194 and MRI53426. Representative Giemsa-stained smears (A) and standard error of the mean (SEM) images (B) of erythrocytes from wild-type (WT; +/+) and both mutant lines. Hematological properties from an automated blood count. (C) Mean cell volume (MCV), mean cell hemoglobin (MCH), RBC (erythrocyte) count, and hemoglobin (HGB) by volume (n = 14-36 per group). (D) Mean values for volume, surface area, ratio of surface area to

A critical aspect of the lifecycle of *Plasmodium* is its interaction with the erythrocyte membrane skeleton, which it manipulates to enter, develop within, and egress from the erythrocyte.[14] Populations in endemic malaria areas have an increased prevalence of mutations in skeletal proteins causing hereditary spherocytosis (HS) or hereditary elliptocytosis (HE).[15,16] Southeast Asian ovalocytosis (SAO), a form of HE caused by a mutation in band 3, is known to reduce rates of cerebral malaria.[17,18] Other studies exploring the potential association of these conditions with malaria risk are lacking. Ankyrin-1 links the spectrin-actin cytoskeleton to the red blood cell (RBC) membrane and band 3 protein. The interaction between ankyrin-1 and spectrin proteins is essential to maintain the integrity of the RBC.[19] The disruption of this interaction affects the rigidity of RBCs and results in conditions such as HS, HE, or SAO.[20] In vitro studies have demonstrated impaired invasion and/or growth in erythrocytes from individuals with HE and HS, indicating a likely role for these mutations in malaria resistance.[21-23] Furthermore, several distinct mutations in ankyrin-1 (*Ank1*) and α spectrin (*Spta1*), associated with HS, have been shown to convey resistance to *P chabaudi* and *P berghei* infection in mice.[24-27] The mechanisms responsible for reduced parasite proliferation in vitro or malaria resistance in vivo are poorly understood in these conditions. The best studied is SAO, where impaired merozoite invasion of erythrocytes has been proposed as a protective mechanism conveyed by this condition. It has been suggested that the loss of merozoite binding partners,[28] increased membrane-skeleton interactions,[29] or membrane rigidity[30] hinders invasion of these cells.

To better understand the contribution of the interaction between spectrins and ankyrin-1 to malaria resistance, we generated and studied 2 novel *N*-ethyl-*N*-nitrosourea (ENU)–induced mutations in the β spectrin gene (*Sptb*) in mice. Mutations in *Sptb* are associated with both HE and HS; however, the influence of mutations in *Sptb* on the course of malaria is unknown. We found ENU-mutated mice had erythrocytes that were slightly reduced in size and deformability. Strikingly, these mice were highly resistant to rodent malaria infection. We showed that this was not due to reduced parasite invasion; rather, infected *Sptb*-mutant erythrocytes had an enhanced susceptibility to clearance by the host or maturation defect. To assess the potential of *Sptb* to influence malaria susceptibility, we mutated a previously identified[31] critical binding site between β spectrin and ankyrin in mice using CRISPR/Cas9 genome editing. These mice also displayed a high level of protection against *P chabaudi* infection, highlighting the influence of *Sptb* in determining malaria susceptibility.

Methods

For detailed descriptions and previously published methods, see supplemental Data.

Mice and ethics

Experiments were performed on SJL/J mice unless otherwise stated. Procedures were in accordance with policies of the Australian National University and National Health and Medical Research Council Australian code of practice approved under Ethics No. AEEC 2014/54.

ENU mutagenesis and linkage mapping of causative mutation

ENU mutagenesis and blood screening were performed as described.[24] Mice received 2 intraperitoneal injections of 150 mg/kg of ENU (Sigma-Aldrich, St Louis, MO), and progeny were screened for peripheral blood parameters using an Advia 120 hematological analyzer (Siemens, Berlin, Germany). Causative mutations were identified by linkage analysis as described.[32]

Erythrocyte measurements

Light microscopy,[32] scanning electron microscopy,[27] osmotic fragility,[32] erythrocyte lifespan,[32] ektacytometry,[33] western blots,[27] and in vitro spleen retention assays[34] were performed as previously described. Microfluidic studies were carried out as detailed in supplementary methods.

IVET assays

In vivo erythrocyte tracking (IVET) assays were performed as described with modifications.[35,36] Briefly, freshly drawn blood was incubated at 4°C for 1 hour in 1 of 3 labeling solutions: 6 or 20 μg/mL of NHS-Atto 633 or 125 μg/mL of Sulfo-LC-NHS-Biotin (Thermo Fisher Scientific, Waltham, MA). Labeled erythrocytes were combined and transfused into host mice IV. In some experiments, host mice were injected with 2 doses of clodronate liposomes (CLs; 40 μg/g) IP 24 hours and IV 12 hours before blood sampling to deplete peritoneal, circulating, and tissue resident cells.[37]

Flow cytometry

For malaria infections and IVET assays, blood samples were prepared and analyzed as described with modifications.[35,36] Samples were collected using a BD LSRFortessa or BD Influx flow cytometer (BD Biosciences, Franklin Lakes, NJ), with analysis performed using FlowJo software (version 10.0.6; Tree Star, Ashland, OR) as described.[35,36]

Phagocytosis assays

Blood was collected from infected mice and labeled with 20 μg/mL of NHS-Atto-633. Resident IP cells were harvested by washing cavities with 10 mL of ice-cold mouse tonicity phosphate-buffered saline as previously described.[38] Harvested cells were combined with labeled cells before being allowed to settle onto slides at 37°C for 30 minutes. Nonadherent cells were removed and bound, and nonphagocytized erythrocytes were lysed in ice-cold water for 30 seconds.

Generation of Sptb^{D1781R} mice using CRISPR/Cas9 genome editing technology

Superovulated SJL/J female mice were mated and embryos collected and microinjected using a Nikon Eclipse Ti platform (Nikon, Tokyo, Japan); 5 ng/μL of px461 circular plasmid[39]

Figure 1. (continued) volume, and distance from channel exit of cell populations for WT (3 mice, 642 cells) and MRI2694 (2 mice, 233 cells) erythrocytes. (E) Osmotic fragility of erythrocytes (n = 8-35 per group). (F) Erythrocyte lifespan (n = 4 per group); dashed line is 50%. (G) Erythrocyte deformability as measured by ektacytometry (n = 3-6 per group). (H) Retention of erythrocytes in an in vitro spleen bead filtration model (n = 7 per group). Mean and SEM are indicated, except for microfluidic results, where standard deviation is indicated. Mann-Whitney *U* test was used to calculate *P* values. **P* < .05, ***P* < .01, ****P* < .001 between MRI26194 and WT. #*P* < .05, ##*P* < .01, ###*P* < .001 between MRI53426 and WT. NS, not significant.

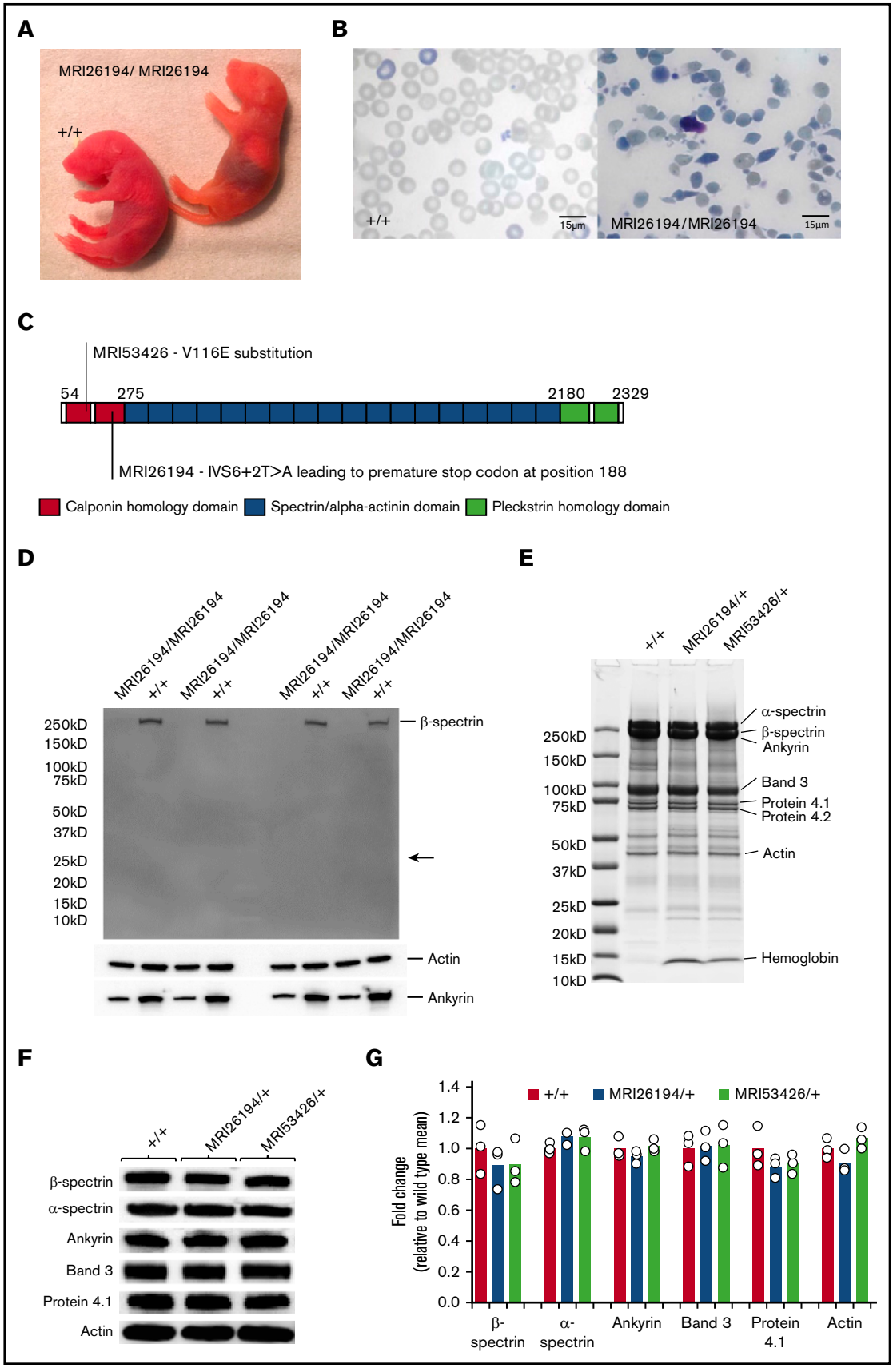
A
MRI26194/ MRI26194
+/+
B
+/+
15μm
MRI26194/MRI26194
15μm
C
MRI53426 - V116E substitution
54
275
2180
2329
MRI26194 - IVS6+2T>A leading to premature stop codon at position 188
Calponin homology domain
Spectrin/alpha-actinin domain
Pleckstrin homology domain
D
MRI26194/MRI26194
+/+
MRI26194/MRI26194
+/+
MRI26194/MRI26194
+/+
MRI26194/MRI26194
+/+
250kD
150kD
100kD
75kD
50kD
37kD
25kD
20kD
15kD
10kD
β-spectrin
Actin
Ankyrin
E
+/+
MRI26194/+
MRI53426/+
250kD
150kD
100kD
75kD
50kD
37kD
25kD
20kD
15kD
10kD
α-spectrin
β-spectrin
Ankyrin
Band 3
Protein 4.1
Protein 4.2
Actin
Hemoglobin
F
+/+
MRI26194/+
MRI53426/+
β-spectrin
α-spectrin
Ankyrin
Band 3
Protein 4.1
Actin
G
+/+
MRI26194/+
MRI53426/+
Fold change
(relative to wild type mean)
1.4
1.2
1.0
0.8
0.6
0.4
0.2
0.0
β-
spectrin
α-
spectrin
Ankyrin
Band 3
Protein
4.1
Actin

Figure 2.

(obtained from Addgene and gifted from Zhang Laboratory, ID 48140) and 20 ng/μL of ultramer single-stranded oligonucleotides (IDT, Singapore) were delivered into fertilized zygotes by pronuclear injection. The microinjected zygotes were surgically transferred into 8- to 12-week-old pseudoplugged CBA/J × SJL/J recipient females. Founder mice were genotyped for the presence of the point mutation using Sanger sequencing.

Statistics

For malaria survival, statistical significance was determined by the Mantel-Cox test. For ratios obtained in the IVET assays, significance was determined using the 1-sample *t* test with 1 as the hypothetical mean. For other results, a 2-tailed Student *t* test was used.

Results

ENU-induced mutations in Sptb in 2 mouse strains with a dominant microcytosis phenotype

We established 2 mouse lines from an ENU mutagenesis screen with a dominant, microcytic inheritance pattern, MRI26194 and MRI53426. Despite being microcytic, erythrocytes exhibited a biconcave shape (Figure 1A-B), and mice displayed no additional pathological phenotypes or infertility. Hematological analysis revealed decreased cellular hemoglobin content; however, this was counteracted by an increased erythrocyte count, so hemoglobin blood levels were normal (Figure 1C). Using an HEMA microfluidics device,[40] we found that both surface area and volume of MRI26194 erythrocytes were decreased compared with WT. The ratio of surface area to volume was slightly decreased for the mutants (Figure 1D). Taken together, this is consistent with the maintenance of the biconcave disc shape. MRI26194 erythrocytes also did not progress as far into the trapping channels (~28% closer to the channel mouth), indicating reduced cellular deformability (Figure 1D). Mutant erythrocytes were significantly more osmotically fragile (Figure 1E) and showed an in vivo half-life reduced by ~25% (Figure 1F). The reduction in mutant-cell deformability was confirmed using ektacytometry (Figure 1G) and resulted in >50% of cells retained in an in vitro spleen-mimic filtration assay (Figure 1H).

We intercrossed microcytic mice to establish a homozygous phenotype. For MRI26194, most offspring resembled the parental or WT erythrocyte phenotype, although a limited number of pups exhibited jaundice and rapid breathing and lived no longer than 48 hours (Figure 2A). Blood smears from these pups revealed severe erythrocyte fragmentation, spherocytic erythrocytes, and reticulocytosis, indicating these mice were likely homozygous (Figure 2B). For MRI53426, offspring displayed only the WT or parental microcytosis phenotype. Embryo reabsorption was evident as early as E9.5, suggesting homozygosity for MRI53426 is lethal early in development.

Linkage mapping and a candidate gene approach lead us to identify an A→T transversion in the exon 6/intron 7 boundary (IVS6+2T>A) of the S*ptb* gene in the MRI26194 line (supplemental Figure 1). This mutation, designated $Sptb^{MRI26194}$, is predicted to disrupt splicing of intron 7 and result in translation of a 188 amino acid residue truncated protein (Figure 2C). In the MRI53426-mutant line, a T→A transversion was identified in exon 4 of *Sptb*. This mutation, $Sptb^{MRI53426}$, results in a valine to glutamic acid missense mutation (V116E; Figure 2C; supplemental Figure 1). The V116 residue is located within the *N*-terminal calponin homology domain, which is involved in binding to erythrocyte β actin.[41] Analysis using the SIFT algorithm indicated this amino acid is also conserved across 46 species, suggesting the V116E mutation may disrupt a critical function.[42] Both mutations completely segregated with the microcytic phenotype over >10 generations, whereas jaundiced pups identified in the MRI26194 line were homozygous for the IVS6+2T>A mutation. Together these indicate a phenotype compatible with that seen for HS or HE in human populations.

mRNA and protein expression in Sptb-mutant mice

To explain the observed phenotype of mutant mice, we investigated the effects of these mutations on messenger RNA (mRNA) and protein expression. For MRI26194, quantitative polymerase chain reaction analysis of embryonic livers from homozygous and heterozygous mice indicated sufficient β spectrin mRNA expression (supplemental Figure 2). However, no full-length or truncated protein was detectable by western blot in protein extracts from the blood of $Sptb^{MRI26194/MRI26194}$ pups, indicating the mutation disrupts protein expression or stability (Figure 2D). To investigate the erythrocyte skeletal composition of the heterozygote mutants, we examined purified erythrocyte ghosts (supplemental Figure 3) by Coomassie blue staining and western blot (Figure 2E-G). No major differences were found in β spectrin abundance or in other major skeletal proteins (Figure 2E-G). However, there were intense bands in Coomassie-stained gels for both mutant samples at approximately 15 kDa, corresponding to α and β globin chains, suggesting increased membrane-bound hemoglobin (Figure 2E). Together these data suggest that although homozygous mice do not express β spectrin protein (in the case of MRI26194), heterozygous mice are able to compensate for the mutated allele and produce erythrocytes with relatively unperturbed skeletal protein content, albeit of smaller size.

$Sptb^{MRI26194/+}$ and $Sptb^{MRI53426/+}$ mice are resistant to rodent malaria infection

Heterozgous *Sptb* mice inoculated with *P chabaudi adami* DS, normally lethal against this parental mouse strain, displayed a significantly altered course of infection compared with WT mice. Parasitemia was lower between days 9 and 12, and peak parasitemia was reduced by >40%. These differences were associated with increased reticulocyte production beginning on day 9 and a substantial increase in resistance. Over 90% of

Figure 2. The MRI26194 and MRI53426 phenotypes are due to mutations in *Sptb*. (A) Mating between $Sptb^{MRI26194/+}$ by $Sptb^{MRI26194/+}$ mice occasionally produced homozygous pups displaying jaundice. (B) Giemsa-stained blood smears from WT and homozygous pups. (C) Schematic of the β spectrin protein indicating different structural domains, and the locations and predicted effects of the mutations identified in the MRI26194 and MRI53426 lines. (D) Western blot of whole RBC lysates from homozygous and WT pups separated by sodium dodecyl sulfate–polyacrylamide gel electrophoresis (SDS-PAGE) on a 4% to 20% gel and probed using an antibody against the *N*-terminal of β spectrin, with actin and ankyrin-1 as loading controls. The expected size of the truncated β spectrin (24 kD) is indicated with an arrow. (E) Representative image of a Coomasie-stained SDS-PAGE gel containing erythrocyte membrane preparations from mutant and WT mice. (F) Images of western blots of major skeletal proteins in erythrocyte membrane preparations from mutant and WT mice. (G) Quantification of protein bands detected by western blot (3 mice per group).

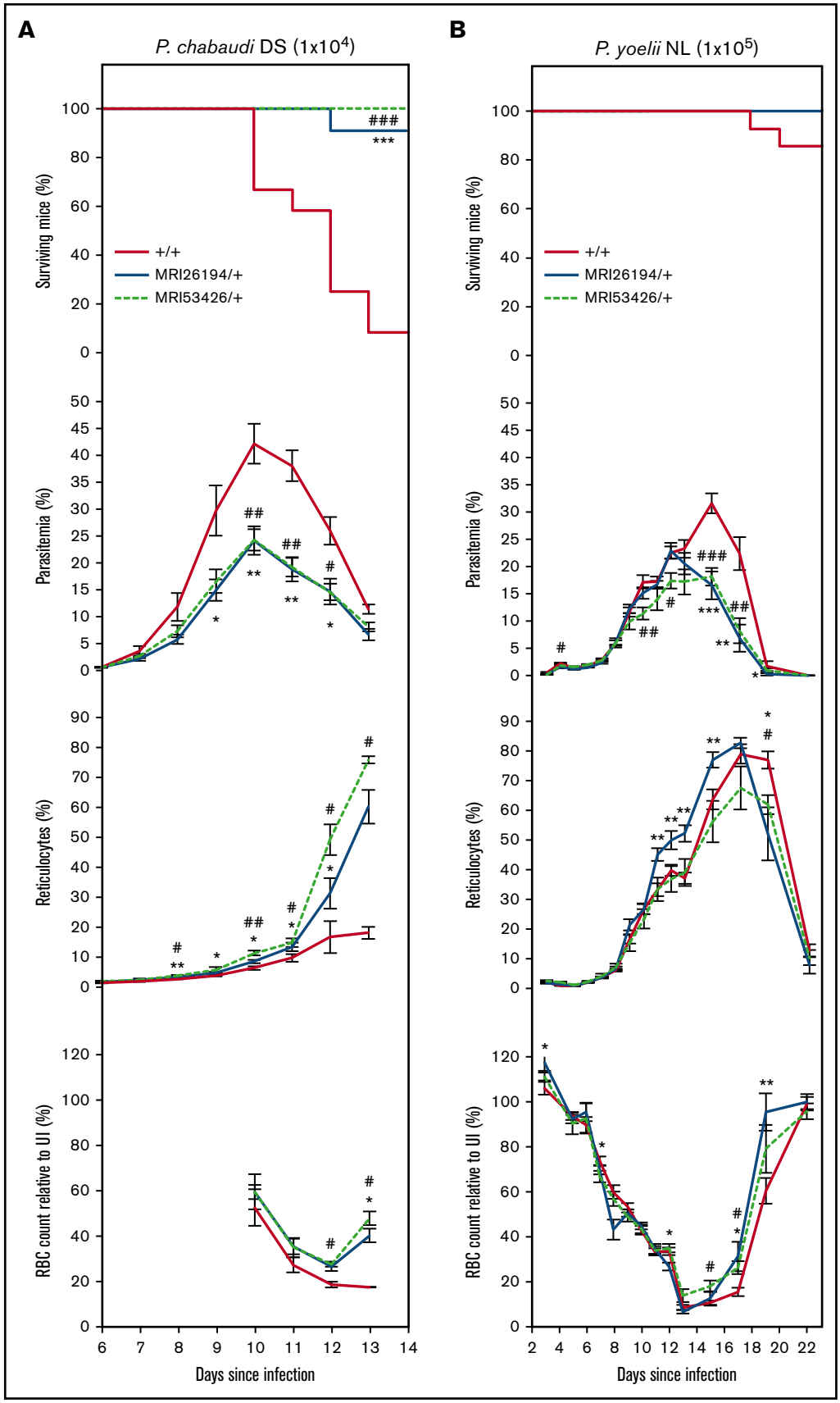
A
P. chabaudi DS (1x10^4)
B
P. yoelii NL (1x10^5)
Surviving mice (%)
+/+
MRI26194/+
MRI53426/+
Parasitemia (%)
Reticulocytes (%)
RBC count relative to UI (%)
Days since infection

Figure 3.

Sptb$^{MRI26194/+}$ mice (10 of 11) and all of the *Sptb*$^{MR53426/+}$ mice (6 of 6) survived the infection, compared with <9% of WT mice (1 of 12; Figure 3A).

Mice were also infected with *P yoelii* NL, which unlike *P chabaudi* has a strong preference for reticulocytes. Except in 2 WT mice that succumbed to infection on days 17 and 19, infection resolved in all other mice. Parasitemia of mutant mice peaked 2 days earlier (day 13; 18% to 23%) and decreased thereafter, whereas in the WT mice, it peaked at approximately 32% on day 15 (Figure 3B). Proportions of infected reticulocytes in all the lines increased rapidly until day 9 before steadily decreasing; the proportion of mutant infected reticulocytes was consistently lower than WT during recovery (supplemental Figure 4). Notably, mutant mice had 43% to 77% fewer infected mature erythrocytes between days 15 and 17 (supplemental Figure 4). Overall, the *Sptb*-mutant lines displayed enhanced resistance to both *P chabaudi* and *P yoelii* infection, characterized by earlier and more rapid clearance of parasites.

Increased clearance of Sptb-mutant erythrocytes during infection

Given the alterations in erythrocyte physiology in the mutant lines, we considered if resistance to *P chabaudi* and *P yoelii* infection was due to an impaired ability of parasites to infect and grow within mutant erythrocytes. To address this, an IVET assay was performed as previously described.[35,36] This assay enables direct comparison of the relative rates of parasite invasion, growth, and clearance in WT vs mutant erythrocytes. Importantly, within this setting, both mutant and WT cells are exposed to the same number of potentially invading merozoites and an identical host response to the infection.

Labeled mutant and WT erythrocytes were transfused into infected WT mice during the peak of schizogony, with labeled and parasitized cells differentiated from host cells by flow cytometry (Figure 4A-B). Because each host animal presents a different set of environmental conditions and level of parasitemia, all results are presented as a ratio relative to WT, with a result of 1 indicating no effect.

Infected labeled cells were detected as soon as 2 minutes after transfusion of WT and mutant erythrocytes in *P chabaudi*–infected host animals, and their frequencies increased during the following 12 hours of monitoring. Relative to WT cells, there were similar or variably higher proportions of newly infected mutant cells (Figure 4Ci). This indicates the rate of merozoite invasion of mutant cells was normal. In contrast, after 3 and 12 hours, the proportion of parasitized mutant cells was smaller than that of WT (15% to 16% and 12% to 17% reduction in *Sptb*$^{MRI26194/+}$ and *Sptb*$^{MRI53426/+}$, respectively). This suggests that once infected, mutant parasitized cells are cleared more rapidly from circulation. Given the smaller volume and increased osmotic fragility of the mutant erythrocytes, this may result from premature rupture of the host cell as the intraerythrocytic parasite develops. Noting that this reduction represents the effect of the mutation over a 24-hour period, we used a mathematical model to predict the consequential effect on parasitemia in the mutant animals over the course of an infection (assuming this difference was similar and additive every 24 hours; supplemental Figure 5). We found this difference was sufficient to entirely account for the parasitemia differences observed in both lines, even at the lowest estimation (12% reduction per 24 hours).

Malaria infection is known to result in accelerated clearance of uninfected erythrocytes, a phenomenon known as the bystander effect.[43] We therefore also compared the relative circulatory lifespan of the WT vs mutant uninfected cells in the infected host animals. We observed 10% to 15% fewer mutant cells 30 minutes after infusion, and this difference was maintained over the 12-hour period of monitoring (Figure 4Cii). Notably, this result was not observed when labeled erythrocytes were transfused into uninfected mice (supplemental Figure 6). Given the increased fragility and decreased deformability of the mutant erythrocytes, it is possible that they are more susceptible to this effect. Overall, both *Sptb* mutations result in an erythrocyte autonomous parasite clearance phenotype, as well as increased bystander cell clearance. We therefore focused additional experiments on identification of the mechanism(s) underlying this phenotype.

Phagocytosis in the spleen is responsible for increased clearance of Sptb-mutant erythrocytes

The spleen plays a central role in malaria immunity[44]; in particular, it selectively removes parasitized cells and directs the development of secondary immune responses. This occurs both through the filtration of poorly deformable cells in splenic endothelial slits and through phagocytosis by resident macrophages. To test if splenic filtration and/or splenic phagocytosis were required for the cell-clearance phenotype, the IVET assay was repeated using splenectomized host mice, which lack splenic filtration and splenic phagocytosis abilities, and mice treated with CLs, which have been depleted of splenic as well as nonsplenic phagocytic cells. Neither the removal of the spleen nor CL treatment had an effect on the elevated clearance of infected mutant cells (Figure 5Ai-Bi). In line with this result, splenectomized *Sptb*$^{MRI26194/+}$ mice infected with *P chabaudi* displayed reduced parasitemia vs splenectomized WT mice (Figure 5C). However, during the IVET assays, the clearance of all labeled mutant cells (infected or not) was equal to or less than that of WT (Figure 5Aii-Bii). This was in contrast to the previous IVET assays, performed with intact host mice. This indicates that inhibition of phagocytosis alone can prevent the preferential bystander clearance of uninfected mutant cells.

The spleen can selectively remove parasitized cells based on decreased cellular deformability.[44,45] We observed that compared with WT erythrocytes, there was greater retention of uninfected mutant erythrocytes in the in vitro splenic bead filtration assay (Figure 1H). In separate experiments, we compared the relative retentions of both infected and uninfected red cells from WT and mutant animals infected with *P chabaudi*. Interestingly, despite a similar increased retention of uninfected mutant cells, passage of

Figure 3. The MRI26194 and MRI53426 *Sptb*-mutant lines are resistant to *P chabaudi adami* DS and *P yoelii* NL infection. Mice were infected with either *P chabaudi* (1×10^4 parasites; 7-12 mice per group) (A) or *P yoelii* (1×10^5 parasites; 8-15 mice per group) (B). Cohorts were analyzed for survival, percentage infected blood cells (parasitemia), percentage of reticulocytes, and RBC count (as a percentage of RBC count in uninfected mice). Mean and standard error of the mean are indicated. The log-rank (Mantel-Cox) test was used to calculate *P* values for survival; Mann-Whitney *U* test was used otherwise. **P* < .05, ***P* < .01, ****P* < .001 between Sptb$^{MRI26194/+}$ and WT. #*P* < .05, ##*P* < .01, ###*P* < .001 between Sptb$^{MRI53426/+}$ and WT.

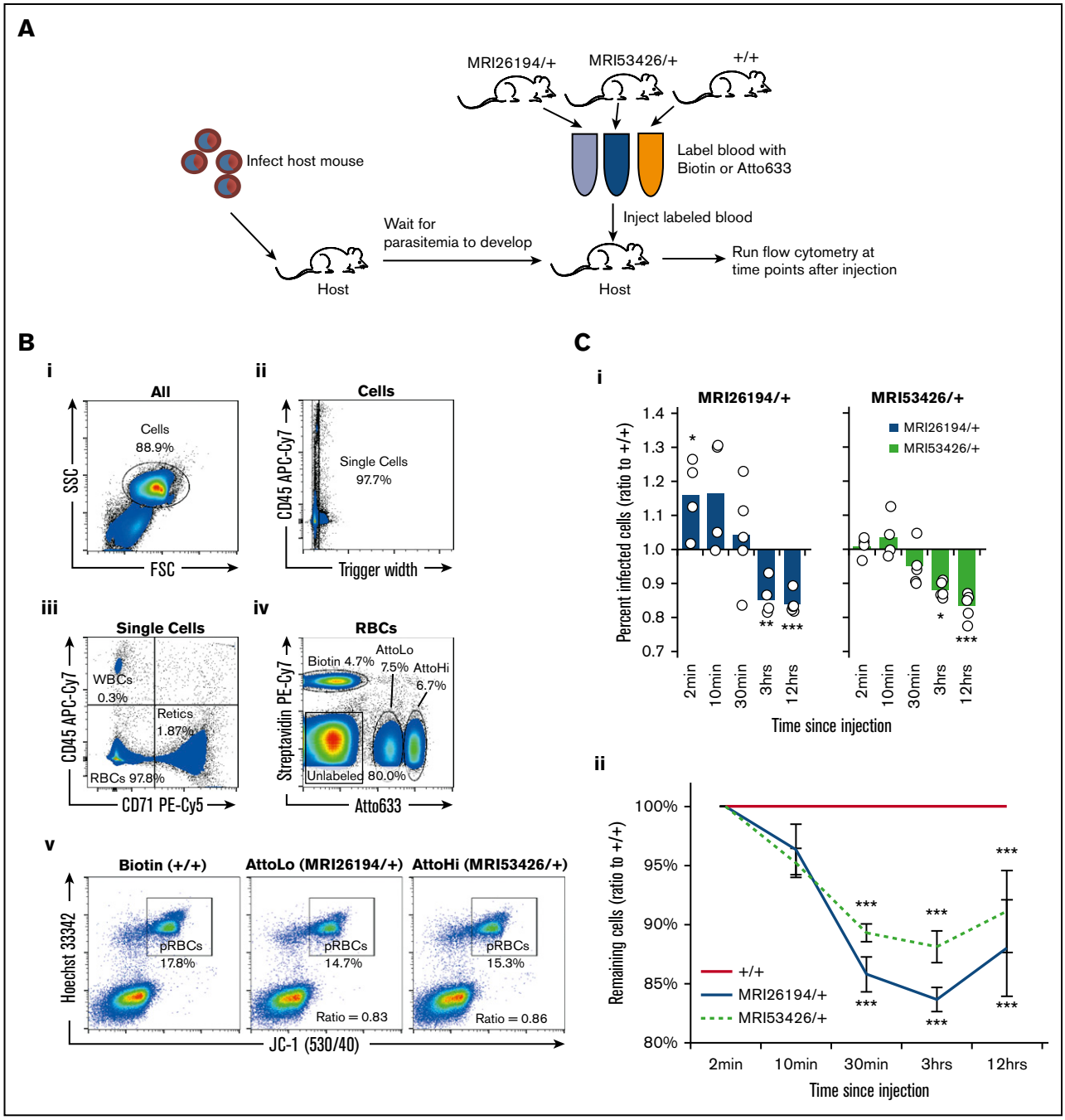

Figure 4. An IVET assay indicates normal invasion but increased clearance of *Sptb*-mutant erythrocytes. (A) Host mice were infected with 1×10^4 *P chabaudi* parasites. At day 9 to 10 of infection, at the peak of schizogony, labeled blood from the 2 mutant lines and WT (+/+) mice was transfused into host mice (n = 5). Labels were switched to account for any dye effects. (B) Representative flow cytometry plots from a host blood sample are shown. Gating of whole cells (Bi), single cells (Bii), mature RBCs (Biii), and the 3 labeled cell populations (Biv) was performed, with other populations removed from analysis. The percentage of infected cells in each population was determined by JC-1/HO dual positive staining (Bv). The percentage of infected cells (ratio to +/+) was determined by dividing the percentage of infected cells (labeled mutant) by percentage of infected cells (labeled WT) in each host animal (in the example plot, for MRI26194/+, the ratio is 14.7/17.8 = 0.83) (Ci). Remaining cells (ratio to +/+) were determined by dividing the percentage remaining of all labeled mutant cells (compared with 2-minute time point) by the proportion remaining of all labeled donor WT cells in each host animal (Cii). A 1-sample *t* test was used between the sample values and the hypothetical value of 1 to test for ratio significance. $^*P < .05$, $^{**}P < .01$, $^{***}P < .001$. pRBC, parasitized RBC; WBC, white blood cell.

infected mutant cells through the filtration column was no different from that of WT (Figure 6Ai-ii). To confirm the susceptibility of mutant cells to phagocytosis, we next performed an in vitro phagocytosis assay. Erythrocytes were collected from *P chabaudi*–infected mice (*Sptb* mutant vs WT). Interestingly, frequencies of phagocytized erythrocytes from both mutant lines were more than

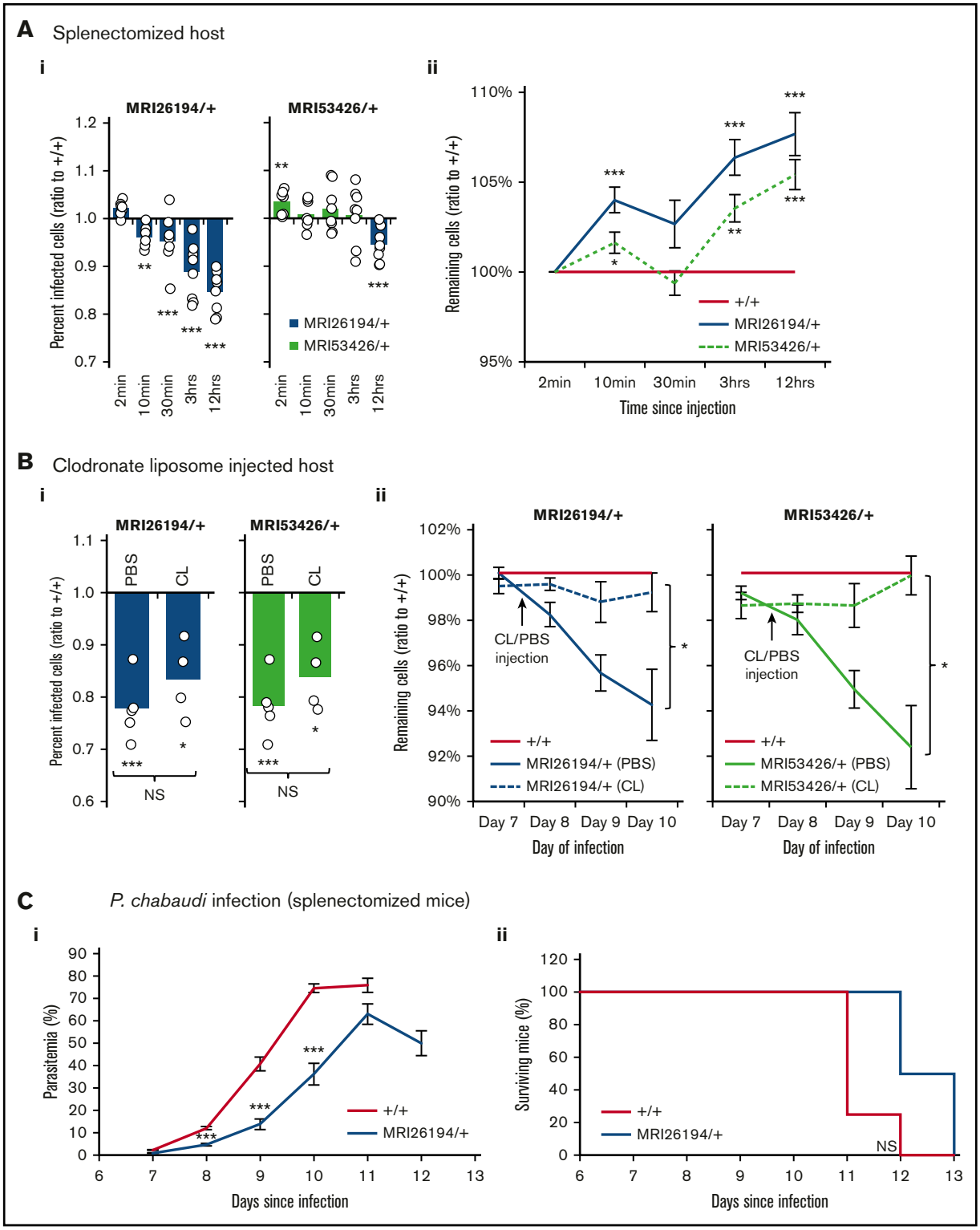

Figure 5. Splenectomy or CL treatment prevents clearance of *Sptb*-mutant erythrocytes. IVET assay results (as described in Figure 4) in splenectomized host animals (8 mice) (A), and host mice injected with phosphate-buffered saline (PBS; n = 4) or CL (n = 4) (B). Percentage of infected cells (ratio to +/+) (Ai) and remaining cells (ratio to +/+) (Aii) in splenectomized mice. Percentage of infected cells (ratio to +/+) on day 10 of infection in PBS- and CL-injected host mice (Bi), and remaining cells (ratio to +/+) after PBS/CL injection (Bii). Parasitemia (Ci) and survival (Cii) of splenectomized WT and $Sptb^{MRI26194/+}$ mice infected with 1×10^4 *P chabaudi* parasites (7-8 mice per group). Mean and standard error of the mean are indicated. The 1-sample *t* test was used to calculate *P* values for ratios; Mann-Whitney *U* test was used otherwise. **P* < .05, ***P* < .01, ****P* < .001.

double those of the WT cells, and this difference was statistically significant (P = .023 and .016 for $Sptb^{MRI26194/+}$ and $Sptb^{MRI53426/+}$, respectively; Figure 6Bii); however, erythrocytes isolated from uninfected mutant and WT mice were rarely internalized, irrespective of *Sptb* allele (Figure 6Bii). We considered if phagocytosis was due to enhanced eryptosis or erythrocyte senescence; however, we found no major differences in terms of phosphatidylserine exposure, calcium flux, C3 binding, immunoglobulin G binding, or band 3 aggregation in mutant cells (supplemental Figure 7). Overall, this supports the hypothesis that *Sptb*-mutant erythrocytes have an inherent susceptibility to phagocytosis during malaria infection, in addition to their decreased RBC deformability and spleen retention.

CRISPR/Cas9-generated mouse line $Sptb^{D1781R/D1781R}$ with a mutation in the ankyrin binding site of β spectrin is resistant to malaria

Our results indicated that 2 distinct mutations in *Sptb* could positively influence the course of malaria infection. A key function of β spectrin in the erythrocyte skeletal matrix is its link to ankyrin-1, facilitated by a small binding pocket between the ZU5 domain of ankyrin-1 and spectrin repeats 14-15.[31] Therefore, we hypothesized that the disruption of this binding in vivo may convey malaria resistance. We used CRISPR/Cas9 to target the aspartate 1781 residue demonstrated previously to disrupt the binding between ANK1 and SPTB.[46] We successfully induced a dinucleotide mutation of GA to CG at this position, causing a substitution with arginine (supplemental Figure 8A). Mice homozygous for this mutation ($Sptb^{D1781R/D1781R}$) displayed a similar hematological phenotype to the ENU-mutagenized lines, confirming the importance of this residue in the erythrocyte skeleton matrix (supplemental Figure 8B-D). Importantly, mice exhibited normal fertility and lived for >18 months without displaying any additional pathological phenotypes or signs of toxicity. When challenged with *P chabaudi*, >70% of $Sptb^{D1781R/D1781R}$ mice survived, whereas all WT mice succumbed to infection (Figure 7Ai). $Sptb^{D1781R/D1781R}$ mice also had reduced parasitemia, increasing more slowly and peaking approximately 30% lower than that in WT littermates (Figure 7Aii). We performed the IVET assay using blood collected from $Sptb^{D1781R/D1781R}$ mice and WT littermates and found that, as was the case for the ENU lines, mutant mice had a significantly reduced proportion of parasitized erythrocytes, which again only occurred 1+ hours postinjection, indicating an increased clearance of parasitized mutant cells compared with WT (Figure 7Bi). However, in contrast to the ENU mutants, no bystander effect was observed; rather, mutant erythrocytes had a prolonged lifespan compared with WT (Figure 7Bii).

Discussion

This study presents 3 key findings. First, 2 distinct ENU-induced mutations in the murine erythrocyte gene *Sptb* conveyed a substantial degree of resistance to *P chabaudi adami* DS and significantly reduced parasitemia during *P yoelii* NL infection. Second, parasite invasion of mutated cells was likely unaffected; however, the clearance of parasitized mutant erythrocytes was enhanced. Third, a targeted amino acid residue change within the ankyrin binding site of β spectrin was also able to convey protection to *P chabaudi* infection, without major adverse effects. Despite this

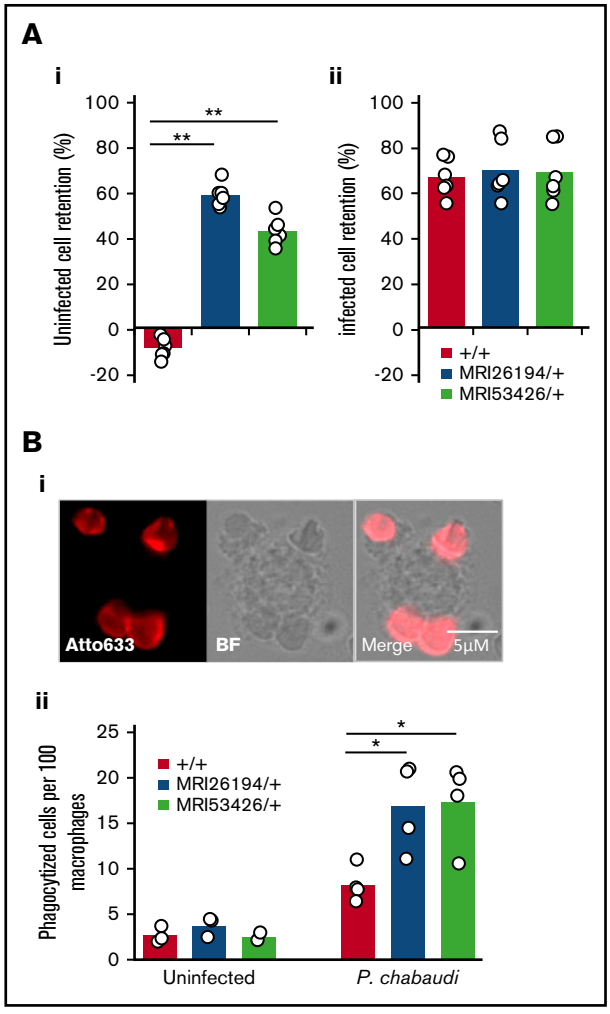

Figure 6. *Sptb*-mutant erythrocytes are more susceptible to retention in an in vitro filtration model and macrophage phagocytosis. Relative retention rates of uninfected (Ai) or infected (Aii) mutant cells compared with uninfected WT cells in an in vitro spleen retention bead assay. Phagocytized cells quantified by fluorescent label (atto633) and macrophages by bright field (Bi-ii). Mann-Whitney *U* test was used to calculate *P* value. *$P < .05$, **$P < .001$.

evidence, we were unable to identify a clear mechanism of malaria resistance or RBC clearance.

Relatively few studies have explored the potential mechanisms by which changes in the host erythrocyte membrane skeleton may affect malaria susceptibility. A prevailing view is that parasite invasion is impeded by skeletal abnormalities.[22,23,47] However, our results indicate this is unlikely to be the basis for the resistance phenotype observed in our study. We observed variably increased or equivalent rates of merozoite invasion in IVET assays. Instead, our IVET analyses allowed us to dissect 2 distinct phenomena that may contribute to the mechanism of resistance. The first is the increased susceptibility of parasitized mutant cells to be cleared from the circulation (12% to 17% increase over 12 hours) because of early maturation arrest or decreased deformability, which plausibly explains the observed reduction in parasitemia over the course of infection as indicated by modeling studies (supplemental Figure 5). Importantly, splenectomy did not affect

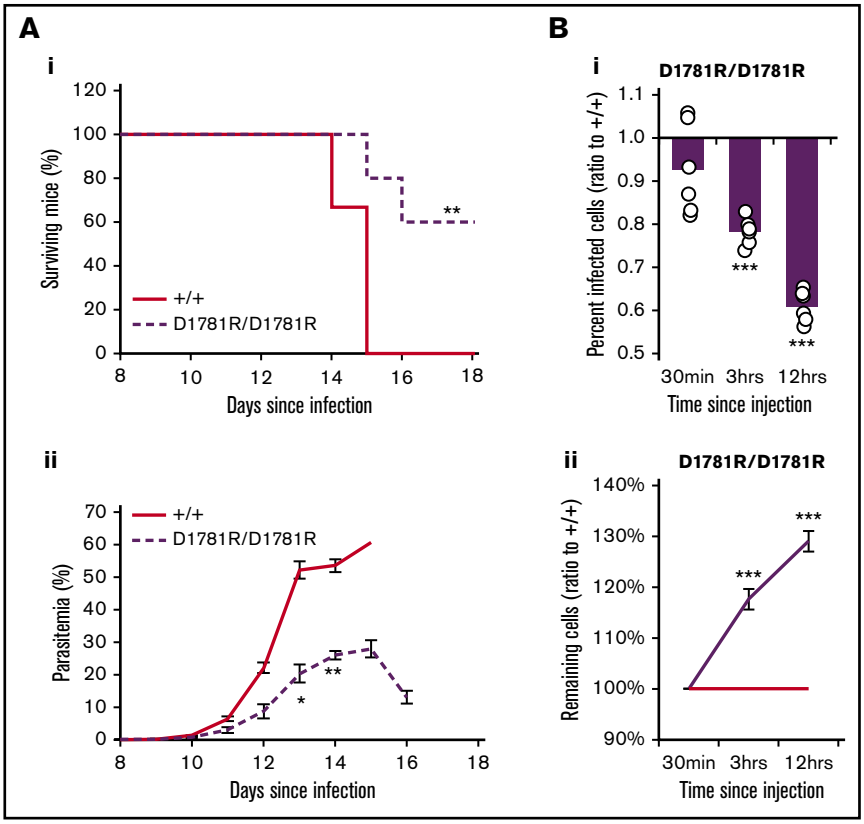

Figure 7. Mice with a targeted CRISPR mutation in the ankyrin binding site of β spectrin are resistant to malaria. Survival (Ai) and parasitemia (Aii) of WT and Sptb$^{D1781R/D1781R}$ mice infected with 1×10^4 *P chabaudi* parasites. (B) IVET assay results (as described in Figure 4) using Sptb$^{D1781R/D1781R}$- and WT-labeled erythrocytes. Percentage of infected cells (ratio to +/+) (Bi) and remaining cells (ratio to +/+) (Bii). Mean and standard error of the mean are indicated. The 1-sample *t* test was used to calculate *P* values for ratios; Mann-Whitney *U* test was used otherwise. $^*P < .05$, $^{**}P < .01$, $^{***}P < .001$.

the preferential clearance of infected cells measured in the IVET assays, indicating a different mechanism is at play compared with the bystander effect. It seems plausible that parasites have a growth defect within mutant erythrocytes, rendering them more susceptible to clearance or inducing premature rupture of the host cell; however, the mechanism of this clearance or maturation defect remains elusive and would require a comprehensive investigation of *P chabaudi* or *P berghei* parasite using microscopy techniques and intravital imaging. This investigation would be complemented by the assessment of the mechanisms of resistance to *P falciparum* from blood of patients with HS or HE carrying Sptb mutations.

The second finding from our analyses is the preferential disappearance of uninfected mutant cells. This phenomenon, called the bystander effect, is a well-known and major contributing factor to severe malarial anemia. Here, we demonstrated the spleen and macrophages are largely responsible; removal of the organ or these cells abrogated the effect. The mechanism of cell clearance may be related to the increased fragility, smaller size, and decreased deformability of the mutant cells. Notably, mutations in skeletal proteins causing HS or HE are known to result in loss of surface area[48] and reduced erythrocyte deformability, and in severe cases, they cause spleen sequestration and reduced erythrocyte lifespan.[48] It seems plausible that during malaria infection, this effect would be intensified, although this is the only study to date that specifically demonstrates the role of the spleen in the bystander clearance of abnormal erythrocytes during malaria.

A major function of β spectrin is its linking of the underlying membrane skeleton to the cell membrane through binding to ankyrin. Using CRISPR/Cas9 genome editing technology, we were able to substitute an aspartate for arginine amino acid in the small ankyrin binding pocket of β spectrin. We showed not only that this mutation disrupts erythrocyte stability and deformability as predicted, but also that homozygous mice were partially protected against *P chabaudi* infection. Together with the ENU-mutant lines, this result indicates allelic heterogeneity at the *Sptb* locus, influencing malaria susceptibility, and highlights the importance of *Sptb* in the host response to malaria. Importantly, disruption of the β spectrin/ankyrin binding site through the D1781R mutation, even in the homozygous case, did not result in any adverse effects, and mice were able to live and breed normally.

Given the findings of this study, it is of interest to determine if naturally occurring mutations in *SPTB* may occur more frequently in malaria-exposed human populations. Several genome-wide association studies have aimed to identify genes associated with malaria risk. Although *SPTB,* associated with HE and HS, was included in 1 of these studies,[49] it was not significantly associated with changes in the occurrence of severe malaria episodes. The lack of association may be due to several reasons, including heterogeneity across study sites, insufficient sensitivity, or population stratification, and more carefully designed studies should be performed before a conclusion can be reached regarding the association between *SPTB* and malaria resistance in humans.

In conclusion, 2 novel ENU-induced mutations in the erythrocyte skeletal gene *Sptb* are reported that protect against malaria. In contrast to previous studies of erythrocyte membrane skeleton mutations, parasites were able to invade mutant erythrocytes normally; however, parasitized erythrocytes were more susceptible

to clearance. This phenotype was reproduced in mice with a homozygous CRISPR/Cas9 mutation in the ankyrin binding site of β spectrin.

Acknowledgments

The authors acknowledge Shelley Lampkin and Emmaline Brown for assistance in the generation of the CRISPR mice, maintenance of mouse colonies, and performance of malaria infection and Preethi Mayura-Guru for assistance in hematological analysis of mice. The authors also thank Ian Cockburn for supplying *P yoelii* parasites and P. V. S. Lee for help with microchip design.

This work was supported by the National Health and Medical Research Council (grants APP605524, 490037 and 1047082), the Australian Research Council (grants DP12010061 and FL150100106), the National Collaborative Research Infrastructure Strategy of Australia and the education investment fund from the Department of Innovation, Industry, Science and Research via the Australian Phenomics Network, and the Japan Society for the Promotion of Science Fellowship Program (grant S16706). This work was performed in part at the Melbourne Centre for Nanofabrication in the Victorian node of the Australian National Fabrication Facility. P.M.L. was a recipient of an Australian post-graduate award.

Authorship

Contribution: P.M.L., H.M.H., B.J.M., S.J.F., and G.B. were responsible for conceptualization; P.M.L., H.M.H., B.J.M., A.N., A.J.B., S.J.F., and G.B. were responsible for methodology; P.M.L., H.M.H., A.N., A.J.B., M.W.D., and G.B. performed investigations; P.M.L. and G.B. wrote the original draft; H.M.H., M.W.D., C.C., L.T., V.R., B.J.M., S.J.F., and G.B. reviewed and edited the manuscript; B.J.M., S.J.F., and G.B. were responsible for funding acquisition; C.C., L.T., and V.R. provided resources; and B.J.M., S.J.F., and G.B. provided supervision.

Conflict-of-interest disclosure: The authors declare no competing financial interests.

The current affiliation for P.M.L. is Laboratory of Malaria Immunology, Immunology Frontier Research Center, Osaka University, Osaka, Japan.

Correspondence: Patrick M. Lelliott, Laboratory of Malaria Immunology, Immunology Frontier Research Center (IFReC), Osaka University, Osaka 565-0871, Japan; e-mail: plelliott@ifrec.osaka-u.ac.jp; and Gaetan Burgio, Department of Immunology and Infectious Disease, John Curtin School of Medical Research, Australian National University, Canberra, ACT 2601, Australia; e-mail: gaetan.burgio@anu.edu.au.

References

1. Kwiatkowski DP. How malaria has affected the human genome and what human genetics can teach us about malaria. *Am J Hum Genet*. 2005;77(2):171-192.
2. Verra F, Mangano VD, Modiano D. Genetics of susceptibility to Plasmodium falciparum: from classical malaria resistance genes towards genome-wide association studies. *Parasite Immunol*. 2009;31(5):234-253.
3. Lelliott PM, McMorran BJ, Foote SJ, Burgio G. The influence of host genetics on erythrocytes and malaria infection: is there therapeutic potential? *Malar J*. 2015;14:289.
4. Wertheimer SP, Barnwell JW. Plasmodium vivax interaction with the human Duffy blood group glycoprotein: identification of a parasite receptor-like protein. *Exp Parasitol*. 1989;69(4):340-350.
5. Horuk R, Chitnis CE, Darbonne WC, et al. A receptor for the malarial parasite Plasmodium vivax: the erythrocyte chemokine receptor. *Science*. 1993;261(5125):1182-1184.
6. Lobo CA, Rodriguez M, Reid M, Lustigman S. Glycophorin C is the receptor for the Plasmodium falciparum erythrocyte binding ligand PfEBP-2 (baebl). *Blood*. 2003;101(11):4628-4631.
7. Cholera R, Brittain NJ, Gillrie MR, et al. Impaired cytoadherence of *Plasmodium falciparum*-infected erythrocytes containing sickle hemoglobin. *Proc Natl Acad Sci USA*. 2008;105(3):991-996.
8. Krause MA, Diakite SA, Lopera-Mesa TM, et al. α-Thalassemia impairs the cytoadherence of Plasmodium falciparum-infected erythrocytes. *PLoS One*. 2012;7(5):e37214.
9. Rowe JA, Handel IG, Thera MA, et al. Blood group O protects against severe Plasmodium falciparum malaria through the mechanism of reduced rosetting. *Proc Natl Acad Sci USA*. 2007;104(44):17471-17476.
10. Cappadoro M, Giribaldi G, O'Brien E, et al. Early phagocytosis of glucose-6-phosphate dehydrogenase (G6PD)-deficient erythrocytes parasitized by *Plasmodium falciparum* may explain malaria protection in G6PD deficiency. *Blood*. 1998;92(7):2527-2534.
11. Ayi K, Turrini F, Piga A, Arese P. Enhanced phagocytosis of ring-parasitized mutant erythrocytes: a common mechanism that may explain protection against falciparum malaria in sickle trait and beta-thalassemia trait. *Blood*. 2004;104(10):3364-3371.
12. Cyrklaff M, Sanchez CP, Kilian N, et al. Hemoglobins S and C interfere with actin remodeling in *Plasmodium falciparum*-infected erythrocytes. *Science*. 2011;334(6060):1283-1286.
13. LaMonte G, Philip N, Reardon J, et al. Translocation of sickle cell erythrocyte microRNAs into Plasmodium falciparum inhibits parasite translation and contributes to malaria resistance. *Cell Host Microbe*. 2012;12(2):187-199.
14. Pei X, Guo X, Coppel R, et al. The ring-infected erythrocyte surface antigen (RESA) of Plasmodium falciparum stabilizes spectrin tetramers and suppresses further invasion. *Blood*. 2007;110(3):1036-1042.
15. Glele-Kakai C, Garbarz M, Lecomte MC, et al. Epidemiological studies of spectrin mutations related to hereditary elliptocytosis and spectrin polymorphisms in Benin. *Br J Haematol*. 1996;95(1):57-66.

16. Eng LI. Hereditary ovalocytosis and haemoglobin E-ovalocytosis in Malayan aborigines. *Nature*. 1965;208(5017):1329.

17. Genton B, al-Yaman F, Mgone CS, et al. Ovalocytosis and cerebral malaria. *Nature*. 1995;378(6557):564-565.

18. Liu SC, Zhai S, Palek J, et al. Molecular defect of the band 3 protein in Southeast Asian ovalocytosis. *N Engl J Med*. 1990;323(22):1530-1538.

19. Saito M, Watanabe-Nakayama T, Machida S, Osada T, Afrin R, Ikai A. Spectrin-ankyrin interaction mechanics: a key force balance factor in the red blood cell membrane skeleton. *Biophys Chem*. 2015;200-201:1-8.

20. Mohandas N, Chasis JA, Shohet SB. The influence of membrane skeleton on red cell deformability, membrane material properties, and shape. *Semin Hematol*. 1983;20(3):225-242.

21. Dhermy D, Schrével J, Lecomte MC. Spectrin-based skeleton in red blood cells and malaria. *Curr Opin Hematol*. 2007;14(3):198-202.

22. Schulman S, Roth EF Jr, Cheng B, et al. Growth of Plasmodium falciparum in human erythrocytes containing abnormal membrane proteins. *Proc Natl Acad Sci USA*. 1990;87(18):7339-7343.

23. Chishti AH, Palek J, Fisher D, Maalouf GJ, Liu SC. Reduced invasion and growth of Plasmodium falciparum into elliptocytic red blood cells with a combined deficiency of protein 4.1, glycophorin C, and p55. *Blood*. 1996;87(8):3462-3469.

24. Greth A, Lampkin S, Mayura-Guru P, et al. A novel ENU-mutation in ankyrin-1 disrupts malaria parasite maturation in red blood cells of mice. *PLoS One*. 2012;7(6):e38999.

25. Rank G, Sutton R, Marshall V, et al. Novel roles for erythroid ankyrin-1 revealed through an ENU-induced null mouse mutant. *Blood*. 2009;113(14):3352-3362.

26. Shear HL, Roth EF Jr, Ng C, Nagel RL. Resistance to malaria in ankyrin and spectrin deficient mice. *Br J Haematol*. 1991;78(4):555-560.

27. Huang HM, Bauer DC, Lelliott PM, et al. A novel ENU-induced ankyrin-1 mutation impairs parasite invasion and increases erythrocyte clearance during malaria infection in mice. *Sci Rep*. 2016;6(1):37197.

28. Cortés A, Benet A, Cooke BM, Barnwell JW, Reeder JC. Ability of Plasmodium falciparum to invade Southeast Asian ovalocytes varies between parasite lines. *Blood*. 2004;104(9):2961-2966.

29. Tilley L, Nash GB, Jones GL, Sawyer WH. Decreased rotational diffusion of band 3 in Melanesian ovalocytes from Papua New Guinea. *J Membr Biol*. 1991;121(1):59-66.

30. Mohandas N, Lie-Injo LE, Friedman M, Mak JW. Rigid membranes of Malayan ovalocytes: a likely genetic barrier against malaria. *Blood*. 1984;63(6):1385-1392.

31. Ipsaro JJ, Huang L, Mondragón A. Structures of the spectrin-ankyrin interaction binding domains. *Blood*. 2009;113(22):5385-5393.

32. Lelliott PM, McMorran BJ, Foote SJ, Burgio G. Erythrocytic iron deficiency enhances susceptibility to Plasmodium chabaudi infection in mice carrying a missense mutation in transferrin receptor 1. *Infect Immun*. 2015;83(11):4322-4334.

33. Dearnley MK, Yeoman JA, Hanssen E, et al. Origin, composition, organization and function of the inner membrane complex of Plasmodium falciparum gametocytes. *J Cell Sci*. 2012;125(Pt 8):2053-2063.

34. Deplaine G, Safeukui I, Jeddi F, et al. The sensing of poorly deformable red blood cells by the human spleen can be mimicked in vitro. *Blood*. 2011;117(8):e88-e95.

35. Lelliott PM, Lampkin S, McMorran BJ, Foote SJ, Burgio G. A flow cytometric assay to quantify invasion of red blood cells by rodent Plasmodium parasites in vivo. *Malar J*. 2014;13(1):100.

36. Lelliott PM, McMorran BJ, Foote SJ, Burgio G. In vivo assessment of rodent Plasmodium parasitemia and merozoite invasion by flow cytometry. *J Vis Exp*. 2015; (98):e52736.

37. van Rooijen N, Hendrikx E. Liposomes for specific depletion of macrophages from organs and tissues. *Methods Mol Biol*. 2010;605:189-203.

38. Zhang X, Goncalves R, Mosser DM. The isolation and characterization of murine macrophages. *Curr Protoc Immunol*. 2008;Chapter 14:Unit 14.1.

39. Cong L, Ran FA, Cox D, et al. Multiplex genome engineering using CRISPR/Cas systems. *Science*. 2013;339(6121):819-823.

40. Gifford SC, Frank MG, Derganc J, et al. Parallel microchannel-based measurements of individual erythrocyte areas and volumes. *Biophys J*. 2003;84(1):623-633.

41. An X, Debnath G, Guo X, et al. Identification and functional characterization of protein 4.1R and actin-binding sites in erythrocyte beta spectrin: regulation of the interactions by phosphatidylinositol-4,5-bisphosphate. *Biochemistry*. 2005;44(31):10681-10688.

42. Kumar P, Henikoff S, Ng PC. Predicting the effects of coding non-synonymous variants on protein function using the SIFT algorithm. *Nat Protoc*. 2009; 4(7):1073-1081.

43. Jakeman GN, Saul A, Hogarth WL, Collins WE. Anaemia of acute malaria infections in non-immune patients primarily results from destruction of uninfected erythrocytes. *Parasitology*. 1999;119(Pt 2):127-133.

44. Safeukui I, Correas JM, Brousse V, et al. Retention of *Plasmodium falciparum* ring-infected erythrocytes in the slow, open microcirculation of the human spleen. *Blood*. 2008;112(6):2520-2528.

45. Safeukui I, Buffet PA, Perrot S, et al. Surface area loss and increased sphericity account for the splenic entrapment of subpopulations of *Plasmodium falciparum* ring-infected erythrocytes. *PLoS One*. 2013;8(3):e60150.

46. Ipsaro JJ, Mondragón A. Structural basis for spectrin recognition by ankyrin. *Blood*. 2010;115(20):4093-4101.

47. Kidson C, Lamont G, Saul A, Nurse GT. Ovalocytic erythrocytes from Melanesians are resistant to invasion by malaria parasites in culture. *Proc Natl Acad Sci USA*. 1981;78(9):5829-5832.

48. Safeukui I, Buffet PA, Deplaine G, et al. Quantitative assessment of sensing and sequestration of spherocytic erythrocytes by the human spleen. *Blood*. 2012;120(2):424-430.

49. Malaria Genomic Epidemiology Network. Reappraisal of known malaria resistance loci in a large multicenter study. *Nat Genet*. 2014;46(11):1197-1204.